Molecular Microbiology (2019) 111(5), 1152–1166
doi:10.1111/mmi.14208
First published online 17 February 2019

Use of rare-earth elements in the phyllosphere colonizer *Methylobacterium extorquens* PA1

Andrea M. Ochsner,[1] Lucas Hemmerle,[1] Thomas Vonderach,[2] Ralph Nüssli,[1] Miriam Bortfeld-Miller,[1] Bodo Hattendorf[2] and Julia A. Vorholt[1]*

[1] *Institute of Microbiology, Department of Biology, ETH Zurich, Vladimir-Prelog-Weg 1-5/10, Zurich, 8093, Switzerland.*

[2] *Laboratory of Inorganic Chemistry, Department of Chemistry and Applied Biosciences, ETH Zurich, Vladimir-Prelog-Weg 1-5/10, Zurich, 8093, Switzerland.*

Summary

Until recently, rare-earth elements (REEs) had been thought to be biologically inactive. This view changed with the discovery of the methanol dehydrogenase XoxF that strictly relies on REEs for its activity. Some methylotrophs only contain *xoxF*, while others, including the model phyllosphere colonizer *Methylobacterium extorquens* PA1, harbor this gene in addition to *mxaFI* encoding a Ca^{2+}-dependent enzyme. Here we found that REEs induce the expression of *xoxF* in *M. extorquens* PA1, while repressing *mxaFI*, suggesting that XoxF is the preferred methanol dehydrogenase in the presence of sufficient amounts of REE. Using reporter assays and a suppressor screen, we found that lanthanum (La^{3+}) is sensed both in a XoxF-dependent and independent manner. Furthermore, we investigated the role of REEs during *Arabidopsis thaliana* colonization. Element analysis of the phyllosphere revealed the presence of several REEs at concentrations up to 10 μg per g dry weight. Complementary proteome analyses of *M. extorquens* PA1 identified XoxF as a top induced protein *in planta* and a core set of La^{3+}-regulated proteins under defined artificial media conditions. Among these was a REE-binding protein that is encoded next to a gene for a TonB-dependent transporter. The latter was essential for REE-dependent growth on methanol indicating chelator-assisted uptake of REEs.

Accepted 10 January, 2019. *For correspondence. Email: jvorholt@ethz.ch; Tel. +41-44-632-5524; Fax +41-44-633-1307.

Introduction

Methylotrophy is the ability of microorganisms to grow on reduced one carbon (C1) compounds such as methanol as their sole source of carbon and energy. Methylotrophs are of interest due to their important role in the global carbon cycle (Chistoserdova, 2015) and as hosts for sugar-independent biotechnological production (Schrader *et al.*, 2009; Chistoserdova, 2018). The Alphaproteobacterium *Methylobacterium extorquens* is one of the best studied methylotrophs and its potential for production of value-added chemicals has been demonstrated (Ochsner *et al.*, 2014). The first step of methylotrophy from methanol is the oxidation of methanol to formaldehyde. In *M. extorquens*, this reaction is catalyzed by a methanol dehydrogenase (Mdh) that depends on the cofactor pyrroloquinoline quinone (PQQ) (Anthony and Zatman, 1964). The enzyme MxaFI, which was discovered more than half a century ago, is a hetero-tetramer that carries a Ca^{2+} ion in its active site (Nunn and Lidstrom, 1986; Nunn *et al.*, 1989; Richardson and Anthony, 1992). The *mxaFI* genes are part of an operon with 12 additional genes encoding e.g. a cytochrome and proteins involved in Ca^{2+} ion insertion (Morris *et al.*, 1995; Amaratunga *et al.*, 1997; Toyama *et al.*, 1998). Genome sequencing revealed a close homolog (47% identity) of *mxaF*, termed *xoxF*, but its function remained elusive for a long time (Chistoserdova and Lidstrom, 1997; Schmidt *et al.*, 2010; Chistoserdova and Kalyuzhnaya, 2018).

Surprisingly, XoxF is a rare-earth element (REE)-dependent PQQ-Mdh that contains a REE instead of a Ca^{2+} ion in its active site (Nakagawa *et al.*, 2012; Pol *et al.*, 2014). XoxF lacks a small subunit and is encoded in a *xoxFGJ* gene cluster that is thought to be sufficient for functional production of XoxF (Keltjens *et al.*, 2014). XoxG is a XoxF-dedicated cytochrome *c* (Zheng *et al.*, 2018) and XoxJ is a homolog of MxaJ with a yet unknown function. The discovery of XoxF as a REE-dependent enzyme marks the first description of an enzyme that specifically depends on these elements as a cofactor. The possibility

of REE-dependent biochemistry has been proposed previously, but REE-dependent enzymes were thought not to have evolved due to the low biological availability of REEs (Lim and Franklin, 2004). The REE-dependent enzyme XoxF now serves as a model to study how REEs can be accommodated in an active site (Prejanò *et al*., 2017; Deng *et al*., 2018; Jahn *et al*., 2018; Lumpe *et al*., 2018; McSkimming *et al*., 2018). In addition to the presence of both types of Mdhs, a Ca^{2+}- and a REE-dependent one in model methylotrophs, some bacteria exclusively harbor *xoxF* and may have been missed in past enrichments for methylotrophs in the absence of REEs (Pol *et al*., 2014; Skovran and Martinez-Gomez, 2015).

XoxF enzymes are diverse and can be divided into at least five clades with potentially different biochemical properties (Keltjens *et al*., 2014; Huang *et al*., 2018). After the discovery of the REE-dependent Mdh XoxF, REE-dependent multi-carbon alcohol dehydrogenases were discovered in *M. extorquens* AM1 (Good *et al*., 2016) and subsequently also in the non-methylotroph *Pseudomonas putida* (Wehrmann *et al*., 2017).

The presence of genes encoding for REE-dependent but also Ca^{2+}-dependent alcohol dehydrogenases (Adh) in the same organism provokes the question of how these genes are regulated. Interestingly, the REE-dependent Adh does not only represent an auxiliary second system, but replaces the Ca^{2+}-dependent enzyme in the presence of suitable REEs (Chu and Lidstrom, 2016; Vu *et al*., 2016; Wehrmann *et al*., 2017; Masuda *et al*., 2018). The signaling cascade underlying this regulatory switch in response to REE is only poorly understood so far. Investigation of the REE switch in two methanotrophs showed that cerium and copper affect the transcription of various genes, including *mxa* and *xox* (Gu *et al*., 2016; Gu and Semrau, 2017) and that the two sensor kinases MxaY and MxaB are involved (Chu and Lidstrom, 2016; Chu *et al*., 2016). Furthermore, a multi-omics approach suggests that the presence of REEs alters the redox balance in the methanotroph *Methylomicrobium alcaliphilum* (Akberdin *et al*., 2018). In the non-methylotroph *P. putida*, the switch from the Ca^{2+}-dependent Adh (encoded by *pedE*) to the REE-dependent Adh (encoded by *pedH*) is mediated by the two-component system PedS2 and PedR2 (Wehrmann *et al*., 2018). In *M. extorquens*, the two-component systems MxbDM and MxcQE are implicated in the regulation of the *mxa* gene cluster and mutational analyses suggests that MxcQE is upstream of MxbDM in the cascade (Springer *et al*., 1997). Furthermore, XoxF, in addition to its role as REE-dependent Mdh, is involved in this regulatory cascade in the absence of REEs (Skovran *et al*., 2011). In a recent study in *M. extorquens* AM1, XoxF was also suggested to sense La^{3+} (Vu *et al*., 2016). However, experimental data confirming the role of XoxF as REE-sensor are still lacking.

In light of the potential impact on the environment, especially in REE-contaminated soils and the application potential of REEs (Martinez-Gomez *et al*., 2016), the role of REE-dependent methylotrophy in the environment requires further investigations. Metagenomics and metaproteomics suggest that XoxF plays an important role in the environment (Delmotte *et al*., 2009; Sowell *et al*., 2011; Knief *et al*., 2012; Taubert *et al*., 2015; Gifford *et al*., 2016). A recent co-culture study found XoxF-dependent cross-feeding between a methanotroph and a non-methanotrophic methylotroph (Krause *et al*., 2017). The phyllosphere, comprising the above-ground parts of plants, is one of the largest habitats on Earth. Methylotrophs such as *M. extorquens* are ubiquitous and abundant on leaves (Vorholt, 2012), where they benefit from methanol released during pectin metabolism (Sy *et al*., 2005; Schmidt *et al*., 2010).

Methylobacterium extorquens PA1 emerged not only as a model system for methylotrophy (Nayak and Marx, 2014; Ochsner *et al*., 2017) but also for plant colonization as a representative of the *Arabidopsis thaliana* leaf microbiota (Ryffel *et al*., 2015; Müller *et al*., 2016; Vogel *et al*., 2016), from which it was isolated (Knief *et al*., 2010). Here, we show that the addition of La^{3+} switches the expression from *mxa* to *xox* in a dose-dependent manner in strain PA1 and that La^{3+} can still be sensed in the absence of XoxF. Furthermore, we quantified a selection of REEs *in planta* and examined the effect of phyllosphere colonization on the proteome of *M. extorquens* PA1, which we compared with the response to La^{3+} under defined culture conditions. This approach revealed several new La^{3+}-regulated proteins, a TonB-dependent transporter as well as an ABC transporter required for La^{3+}-dependent growth on methanol.

Results

XoxF is required for La^{3+}-dependent growth on methanol and is essential for the expression of the mxa *gene cluster in* M. extorquens *PA1*

To confirm the presence of an REE-dependent Mdh in *M. extorquens* PA1, we investigated the growth of a strain lacking the gene encoding the large subunit of the Ca^{2+}-dependent Mdh MxaFI (Δ*mxaF*). The strain was not able to grow on methanol unless the REE La^{3+} was present (Fig. 1). In addition to La^{3+}, growth was also supported by cerium (Ce^{3+}), praseodymium (Pr^{3+}) and neodymium (Nd^{3+}), while samarium (Sm^{3+}) only allowed very slow growth (Fig. 2A). The addition of yttrium (Y^{3+}) and the heavier REEs europium (Eu^{3+}), gadolinium (Gd^{3+}) and holmium (Ho^{3+}) did not enable growth, while ytterbium (Yb^{3+}) decreased growth of the wild type. About 5 μM La^{3+} were sufficient for full restoration of growth of a

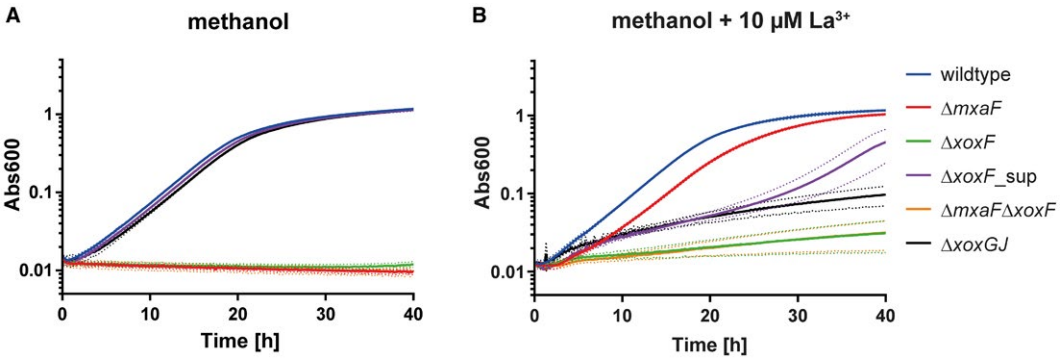

Fig. 1. Growth of wild type, Δ*mxaF*, Δ*xoxF*, Δ*xoxF*_sup, Δ*mxaF*Δ*xoxF* and Δ*xoxGJ* on (A) methanol and (B) methanol with 10 µM La^{3+}, n=4-5. Mean and standard deviation are shown.

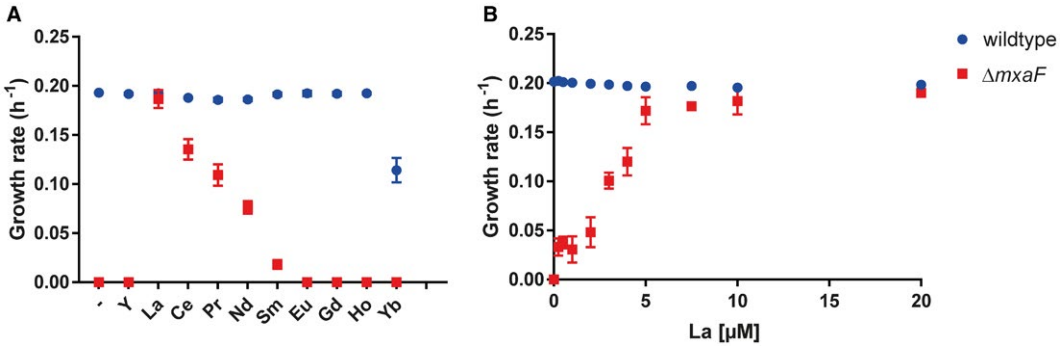

Fig. 2. Growth rates of wild type and Δ*mxaF* on methanol minimal medium with (A) different REEs [10 µM] $n = 4$ or (B) different La^{3+} concentrations, $n = 3–4$. Mean and standard deviation are shown.

Δ*mxaF* strain (Fig. 2B). Deletion of the *xoxF* gene led to an almost complete loss of growth on methanol in the presence of La^{3+} in the *M. extorquens* PA1 strain devoid of *mxaF* (Δ*mxaF*) (Fig. 1). Analogous to strain AM1 (Good *et al*., 2016), the remaining growth is due to the REE-dependent ethanol dehydrogenase ExaF (encoded by Mext_1339) (Fig. S1). Notably, *xoxF* was essential for growth on the standard REE-free methanol medium (thus, in the presence of Ca^{2+} and an intact *mxaF* gene). These findings are overall in line with findings made with strain AM1 (Vu *et al*., 2016). However, the AM1 strain contains two *xoxF* paralogs and only the deletion of both results in a growth deficiency on methanol (Skovran *et al*., 2011).

To further investigate the expression of the two Mdh systems, we analyzed the activities of the promoters P*mxa* and P*xox* in the wild type and the respective deletion strains using a reporter system based on transcriptional *mCherry* fusions. Since the *mxaF* and the *xoxF* deletion strains do not grow on methanol either in the absence and/or presence of La^{3+}, all experiments were carried out in the presence of succinate and methanol. In the wild type strain grown in the absence of La^{3+}, the *mxa* promoter was active, while the *xox* promoter activity was low (Fig. 3A). The expression of P*mxa* and P*xox* was similar in the Δ*mxaF* strain, but changed drastically in the Δ*xoxF* background. In the Δ*xoxF* strain, P*mxa* was turned off (decreased more than 90-fold) and P*xox* was induced (15-fold). These results are in line with findings in strain AM1 (Skovran *et al*., 2011) and suggest that XoxF activates the expression of the *mxa* gene cluster and inhibits the expression of its own gene cluster in the absence of La^{3+} either directly or via other factors.

La^{3+} regulates the expression of the xox *and* mxa *gene clusters in a dose-dependent manner*

The requirement of *xoxF* for La^{3+}-dependent growth on methanol, raises the question of whether P*xox* is induced by La^{3+}. Reporter assays indeed showed that La^{3+} strongly induces P*xox* and at the same time inhibits P*mxa* (Fig. 3A). Closer inspection of the promoter activity with different La^{3+} concentrations showed that roughly 1 µM is required for full activation of P*xox* while roughly 2 µM is sufficient to reduce P*mxa* activity to a minimum (Fig. 3B). At submaximal concentrations, both promoters showed titratability. This mostly agrees with recent findings in strain AM1 (Vu *et al*., 2016), except

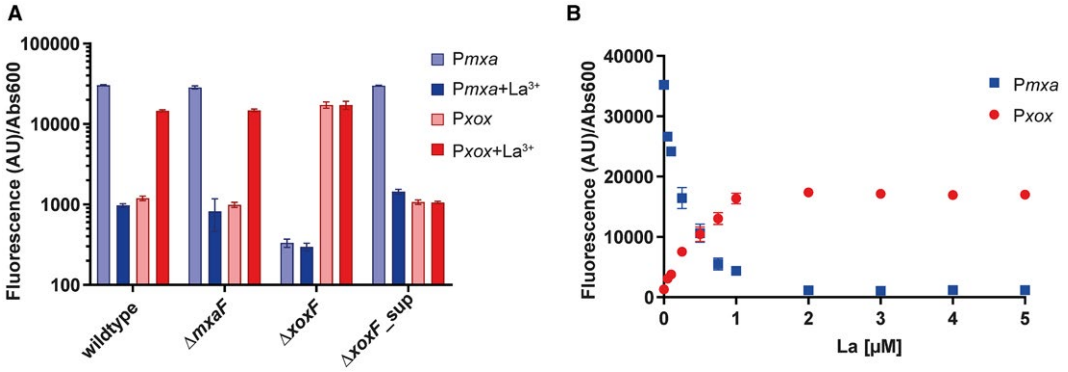

Fig. 3. Promoter activities of P*mxa* & P*xox* in (A) wild type, Δ*mxaF*, Δ*xoxF* and Δ*xoxF*_sup grown in succinate minimal medium containing methanol with and without addition of 10 μM La^{3+}, $n = 4$ or (B) wild type grown in methanol minimal medium containing different amounts of La^{3+}, $n = 3$. Mean and standard deviation are shown.

that roughly four or eight times higher La^{3+} concentrations were required in strain PA1 for full activation of P*xox* or deactivation of P*mxa* respectively. The difference could be strain-specific or due to differences in medium composition, such as the use of distinct chelators. The switch to *xoxF* expression in the presence of La^{3+} implies that the La^{3+}-dependent XoxF is favored over the Ca^{2+}-dependent MxaFI. Moreover, the titratability of P*xox* and P*mxa* suggests that the bacterium adjusts the expression levels of its two Mdh systems in response to the available La^{3+} concentration.

Suppressor mutants of ΔxoxF *occur readily and show restored expression of the* mxa *gene cluster*

As described above, XoxF is involved in the regulation of both the *mxa* gene cluster and its own gene cluster. In order to investigate the signaling cascade further, we looked for spontaneously occurring suppressor mutations that would overcome the effect of a *xoxF* deletion. We identified suppressor mutants after prolonged incubation of Δ*xoxF* on methanol, as previously observed in strain AM1 (Skovran *et al*., 2011). We investigated one of these Δ*xoxF* suppressor mutants (Δ*xoxF*_sup), which showed wild type-like growth on methanol (Fig. 1A) in more detail. To confirm that the suppressor phenotype was due to induction of *mxaFI* expression, activities of P*mxa* and P*xox* were measured. Indeed, P*mxa* activity was restored and the *xox* promoter was not induced in the absence of La^{3+} (Fig. 3A), indicating restored wild type Mdh regulation in Δ*xoxF*_sup. To pinpoint the suppressor mutation(s), we sequenced the genome of Δ*xoxF*_sup. This revealed a duplication of 21 bases (thus seven amino acids without frameshift) in *mxbD* (Mext_1822), encoding the sensor histidine kinase of the two-component system MxbDM (Fig. S2A). Protein sequence analysis of MxbD showed that the duplication in Δ*xoxF*_sup is located at the end of a predicted HAMP (histidine kinases, adenylate cyclases, methyl accepting proteins, phosphatases) domain that is involved in the signal transduction from the periplasmic sensor domain to the cytosolic catalytic domain in other systems (Aravind and Ponting, 1999). Reconstruction of this modified version into a Δ*xoxF* deletion strain resulted in wild type-like growth on methanol (Fig. S2B), confirming that this mutation is indeed causal for the suppressor phenotype.

The suppressor strain provided a unique opportunity to investigate La^{3+} regulation in the absence of XoxF, which was suggested to be the La^{3+}-sensor (Vu *et al*., 2016). This is otherwise challenging due to the requirement of XoxF for the expression of the *mxa* gene cluster and therefore growth on methanol in the absence of La^{3+}. In the Δ*xoxF*_sup strain grown under mixed substrate conditions, P*xox* activity was low in the absence of La^{3+} (see above) and did not increase in the presence of La^{3+} (Fig. 3A). This observation is in line with a phenotype that reverted to wild type and lost responsiveness to La^{3+}. In contrast, P*mxa* activity reached wild type levels in the absence of La^{3+} in the Δ*xoxF*_sup strain. However, the promoter activity was decreased to a minimum in the presence of La^{3+}, showing that La^{3+} is still sensed in absence of XoxF, which suggests a distinct regulatory mechanism for *xox* and *mxa* gene cluster expression. Consequently, Δ*xoxF*_sup showed a growth defect on methanol in the presence of La^{3+} that varied in strength (Figs 1B and S2C), suggesting either the emergence of additional suppressor mutations or metabolic adaptation. Resumed growth on methanol in the presence of La^{3+} indicates regained expression of P*mxa* after prolonged incubation time. Analysis of the promoter activities on methanol in the presence of La^{3+} (and in the absence of succinate) indeed showed increased, but not wild type level, expression of P*mxa* after growth resumed (Fig. S2D).

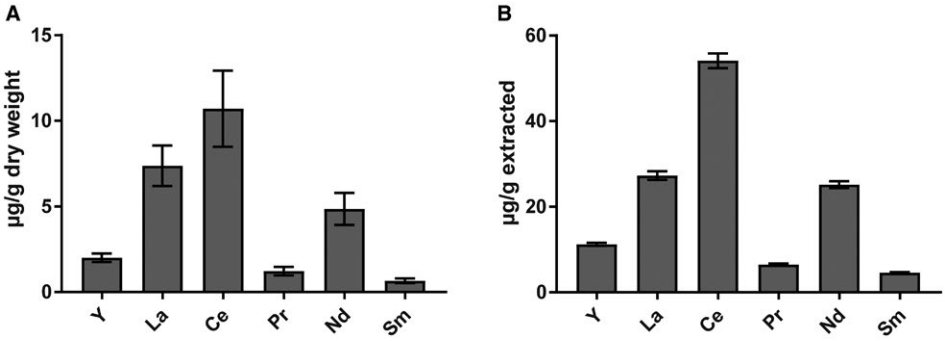

Fig. 4. REE content determined by ICP-MS of (A) the entire phyllosphere of 6-week-old *Arabidopsis thaliana* and (B) extracts of calcined clay used for cultivation, $n = 3$. Mean and standard deviation are shown.

XoxG and XoxJ are required for REE-dependent growth on methanol, but not for expression of the mxa *gene cluster*

As described above, the presence of XoxF is required for the expression of the *mxa* gene cluster and therefore growth on methanol. So far, it remains elusive if the presence of the protein is sufficient or if enzymatic *in vivo* activity is required for a functional regulatory cascade. To address this question, we analyzed the growth phenotype of a strain lacking the two auxiliary genes encoded in the *xox* cluster (Δ*xoxGJ*). Such a mutant strain was able to grow normally in the absence of La^{3+} (Fig. 1A), which is in line with findings in strain AM1 (Chistoserdova and Lidstrom, 1997). In contrast, its growth was strongly impaired in the presence of La^{3+}. Additional deletion of *mxaF* resulted in the same residual growth phenotype as observed for the Δ*mxaF*Δ*xoxF* strain (Fig. S3). This confirms that *xoxGJ* are required for the activity of XoxF *in vivo* and indicates that electron flow from XoxF is neither required for expression of the *mxa* gene cluster nor for sensing of La^{3+}.

REEs are available in the phyllosphere of clay-grown Arabidopsis thaliana

The environmental relevance of MxaFI and XoxF is still poorly understood. *M. extorquens* PA1 was isolated as a competitive *Methylobacterium* strain from the phyllosphere of *A. thaliana* (Knief *et al.*, 2010). To investigate the availability of REEs under controlled conditions *in planta*, we used a gnotobiotic cultivation system relying on calcined clay as an inert growth substrate (Bai *et al.*, 2015; Lebeis *et al.*, 2015). To determine the REE content, the aerial parts of 6-week-old *A. thaliana* plants were lyophilized, processed using wet chemical digestion, and analyzed using inductively coupled plasma mass spectrometry (ICP-MS) (Fig. 4A). We focused on the light REEs yttrium, lanthanum, cerium, praseodymium, neodymium and samarium. All these elements could be detected in the *A. thaliana* phyllosphere. Among them, samarium showed the lowest concentration (0.7 ± 0.1 µg g^{-1} plant dry weight), while cerium was the most abundant (10 ± 2 µg g^{-1}) followed by lanthanum (7 ± 1 µg g^{-1}). To confirm that the clay used for plant cultivation was the main source of REEs in the system, we extracted the clay and found a similar relative distribution of REEs (Fig. 4B).

The response of the proteome to the presence of La^{3+} and the overlap with the in planta *proteome*

To investigate the response of *M. extorquens* PA1 to phyllosphere colonization, we performed a proteomics experiment using the gnotobiotic conditions described above. To identify proteins with higher abundance *in planta*, the proteome of *M. extorquens* PA1 grown *in planta* was compared to the proteome of cells grown on solid minimal medium (without REEs). This approach revealed a total of 321 proteins with significantly (fold change ≥ 4, *q*-value ≤ 0.001) higher abundance *in planta* and 83 proteins with relative higher abundance on plates (of 1824 detected with at least three unique peptides) (Fig. S4, Data set S1). One of the proteins with the highest abundance increase *in planta* was the REE-dependent Mdh XoxF (157-fold). The other two proteins encoded in the cluster also showed significantly higher abundances *in planta*, with fold changes of 12 for XoxG and 19 for XoxJ, which underlines the presence of REE in the phyllosphere.

Because the adaptation of bacteria to *in planta* conditions was, as expected, substantial (Gourion *et al.*, 2006; Müller *et al.*, 2016) and goes beyond the impact of REEs, we then compared cells grown on methanol in the absence and presence of 10 µM La^{3+}. This data set revealed eight proteins that increased in abundance in response to La^{3+} and 16 that decreased (of 1740 proteins detected with at least three unique peptides) (Fig. 5A). The latter include all

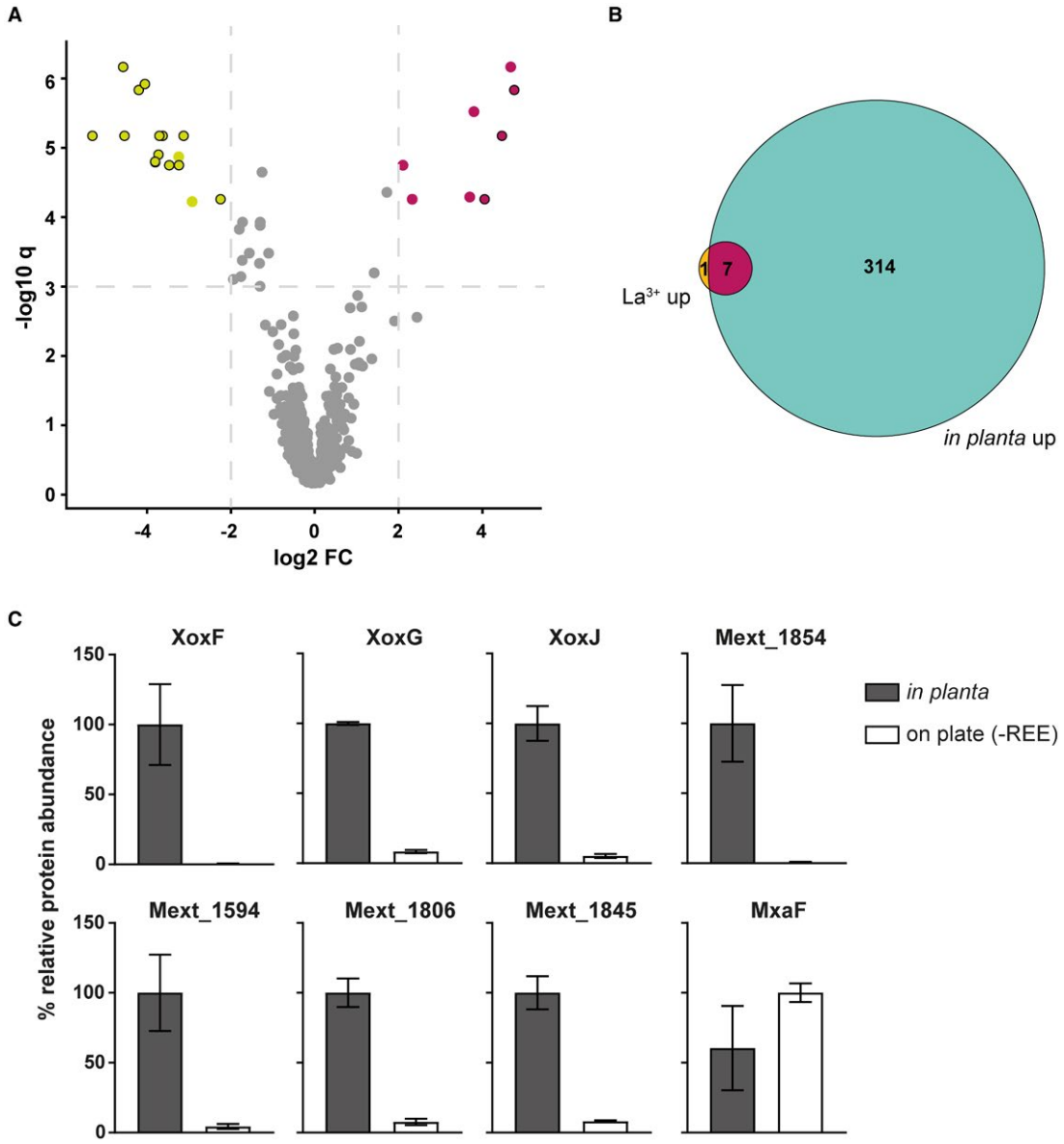

Fig. 5. Proteomics A. Comparison of the proteome of *M. extorquens* PA1 grown in the absence and presence of 10 μM La^{3+}, $n = 5$. Shown is log2-fold change (+La^{3+}/–La^{3+}) with a cutoff of –2/2, q-value ≤ 0.001 for proteins with at least three unique peptides. Mxa and Xox proteins are marked with black edges. B. Overlap of proteins more abundant *in planta* (blue) and more abundant in the presence of La^{3+} (yellow). (C) Relative protein abundance *in planta* and on plate in absence of REEs (shown in percent of the higher relative abundance) of REE-upregulated proteins in addition to MxaF as reference, $n = 3$. Mean and standard deviation are shown.

the 14 proteins encoded in the *mxa* gene cluster and two additional proteins (see Data set S1). For proteins that were more abundant under La^{3+} conditions, we found a high overlap with proteins that were also more abundant upon plant colonization (7 out of 8 proteins) (Fig. 5B and C). Among these seven proteins are XoxF, G and J, while the other four are candidates for La^{3+} uptake, sensing or metabolism (Table 1). The most induced gene upon La^{3+} addition (26-fold) was Mext_1854, which was also among the 15 most induced proteins *in planta* (125-fold). Notably, a recent transcriptome study in *M. aquaticum* also found an induction of the corresponding ortholog by La^{3+} (Masuda *et al.*, 2018). The protein sequence contains putative EF-hand domains, which are known to bind calcium, but also bind lanthanides in some cases (Lim and Franklin, 2004). Indeed, two recent publications confirmed highly selective REE-binding of the ortholog in *M. extorquens* AM1, termed lanmodulin (Cook *et al.*, 2019; Cotruvo *et al.*, 2018). Other regulated proteins include the substrate binding protein of an ABC transporter system encoded next to *xoxFGJ* (Mext_1806), and two hypothetical proteins with predicted signal peptides (Mext_1594 & Mext_1845). However, deletions of the genes

Table 1. Proteins that are more abundant in the presence of La^{3+}. Cutoffs are log2-fold change ≥ 2 and *q*-value ≤ 0.001 and at least three unique peptides. Proteins that are also more abundant *in planta* with the same cutoffs are labeled with a cross in the column 'up *in planta*'.

Locus tag	Description	*q* value	log2FC	up *in planta*
Mext_1163	Hypothetical	5.51E-05	2.32	
Mext_1594	Hypothetical	3.01E-06	3.80	x
Mext_1806	Substrate binding protein of ABC transporter	5.12E-05	3.70	x
Mext_1809	XoxF	6.72E-06	4.46	x
Mext_1810	XoxG	5.51E-05	4.05	x
Mext_1811	XoxJ	1.47E-06	4.76	x
Mext_1845	Hypothetical	1.78E-05	2.10	x
Mext_1854	Lanmodulin (REE-binding protein)	6.83E-07	4.67	x

encoding the three most regulated proteins (Mext_1854, Mext_1806 and Mext_1594) in a Δ*mxaF* background did not result in a growth defect on methanol in the presence of La^{3+} under the tested conditions (Fig. S5A).

The genomic context of the regulated proteins reveals essential transporters

Closer inspection of the genomic context of the genes induced by La^{3+} revealed the presence of TonB-dependent outer membrane receptors encoded next to Mext_1854 (Fig. 6A) and Mext_1594. Mext_1853 did not respond significantly to the presence of La^{3+} at the protein abundance level, while Mext_1595 was only detected with one unique peptide. Growth assays with strains containing the respective deletions in a Δ*mxaF* background revealed that Mext_1853 is strictly required for La^{3+}-dependent growth of Δ*mxaF* on methanol (Fig. 6B), whereas a deletion of Mext_1595 had no effect under the same growth conditions (Fig. S5A). Analysis of a strain defective for Mext_1853 in a wild type background confirmed that the observed phenotype is indeed specific for REE-dependent growth on methanol and not a general growth defect on methanol (Fig. S5B). TonB-dependent transporters are outer membrane importers that rely on the proton motive force that is harnessed by the TonB-ExbB-ExbD complex (Noinaj *et al.*, 2010). They are most well known for the import of iron-loaded siderophores, ensuring iron supply under iron limiting conditions (Hider and Kong, 2010). The uptake of lanthanides by a TonB-dependent mechanism has been hypothesized based on the co-localization with *xoxF* genes in other organisms (Keltjens *et al.*, 2014) and the presence of a putative REE-regulated sequence in the promoter region (Gu *et al.*, 2016). Some members of the TonB-dependent transporter family are also involved in signal transduction via a transmembrane anti-sigma factor and ECF subfamily sigma factor, which are co-localized in many cases (Koebnik, 2005). The absence of putative sigma factors or anti-sigma factors in the proximity of Mext_1853 might therefore suggest that this particular TonB-dependent transporter is not directly involved in signaling. A more detailed characterization showed that Mext_1853 is not only required for La^{3+}-dependent growth of Δ*mxaF*, but also for growth depending on Ce^{3+}, Pr^{3+}, Nd^{3+}, and Sm^{3+} (Fig. S5C). Furthermore, promoter activity assays in the ΔMext_1853 strain showed that both P*mxa* and P*xox* do not respond to the presence of lanthanides (Fig. 6C). This further confirms the central role of Mext_1853 in REE metabolism and suggests that La^{3+} is sensed either in the periplasm or cytosol following uptake by Mext_1853.

Due to the low solubility of REEs under environmental conditions (Firsching and Brune, 1991) as exemplified by complex formation with phosphate, it is likely that REEs are solubilized by a chelator before being imported. In addition, the vast majority of known substrates of TonB-dependent receptors are either organic molecules or metal ions bound to chelators (Schauer *et al.*, 2008). In many cases, the biosynthetic machinery of the chelator is encoded in the proximity of the TonB-dependent transporter (Wandersman and Delepelaire, 2004). Inspection of the genomic region of Mext_1853 revealed no obvious candidates for the biosynthesis of a chelator, but the presence of an ABC transport system (Fig. 6A) that is homologous to a system that is involved in 2-phenylethanol metabolism in *P. putida* (Arias *et al.*, 2008). In the genome of *M. extorquens* PA1, the encoding genes are separated by two genes encoding hypothetical proteins, one of which has a putative cupredoxin-fold. Mutants were generated in the Δ*mxaF* background lacking either the first two genes of the transport system (ΔMext_1846-7) or the two other genes of the transport system and the two hypotheticals (ΔMext_1848-51). Δ*mxaF*ΔMext_1846-7 showed a severe growth defect while Δ*mxaF*ΔMext_1848-51 showed a complete lack of growth on methanol in the presence of La^{3+} (Fig. 6B). Both deletions in the wild type background did not lead to a growth defect on methanol (Fig. S5B), confirming a specific role in REE-dependent

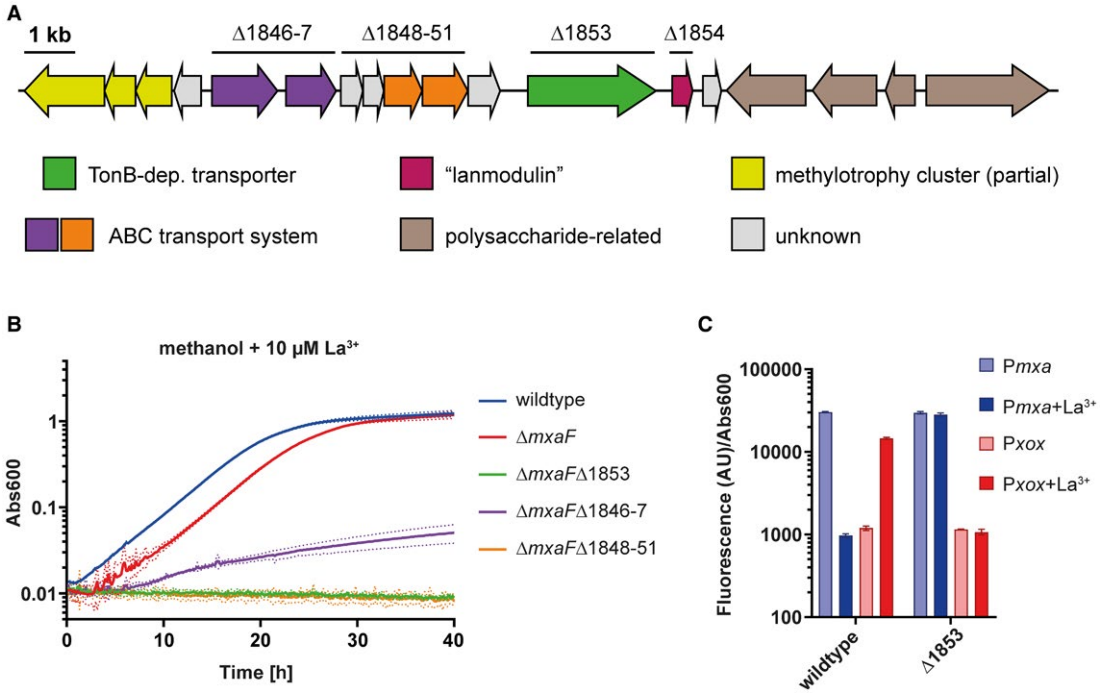

Fig. 6. A. Genomic context of Mext_1853. The region upstream encodes for the largest 'methylotrophy island' of strain PA1, containing various genes involved in one-carbon metabolism including the *xox* cluster (only shown partially). B. Growth of deletion strains of neighbors of top regulated candidates in Δ*mxaF* background on methanol medium with 10 µM La^{3+}, $n = 4$. Mean and standard deviation are shown. C. Promoter activities of P*mxa* & P*xox* in wild type and ΔMext_1853 grown in succinate minimal medium containing methanol with and without addition of 10 µM La^{3+}, $n = 4$.

methylotrophy. Further dissection of the genes in this cluster will be required to probe the contribution of each gene to the observed phenotype. Based on the presence of a periplasmic-binding protein (Mext_1846), the ABC transporter is most likely an importer (Beek *et al.*, 2014). This suggests that La^{3+} actually enters the cytosol, in spite of its known function in the periplasm (refer to Fig. 7 for an overview).

Discussion

In this study, we showed that *M. extorquens* strain PA1 is able to grow on methanol in the presence of the REE La^{3+} in the absence of a functional MxaFI enzyme. XoxF is responsible for the observed growth and involved in the regulation of both the *mxa* gene cluster and its own gene cluster. These data are in line with findings made with strain AM1, which – in contrast to strain PA1 – contains two XoxF paralogs (Skovran *et al.*, 2011; Nakagawa *et al.*, 2012; Vu *et al.*, 2016). In the presence of La^{3+}, gene expression switches from *mxa* to *xox* in a dose-dependent manner. This implies that the La^{3+}-dependent XoxF is favored over the Ca^{2+}-dependent MxaFI and that the bacterium tunes the expression level of its two Mdh systems in response to the available La^{3+} concentration.

To date, it is not well understood how the La^{3+}-dependent regulation of Mdh expression is achieved. A recently published model suggests XoxF as a La^{3+} sensor. In its inactive form (no La^{3+} bound), it might serve as an activating signal sensed by the sensor kinase MxcQ, which leads to the activation of *mxa* expression (Vu *et al.*, 2016). Direct evidence for the role of XoxF as La^{3+} sensor is difficult to obtain due to the essentiality of *xoxF* even in the absence of La^{3+} and because of the effect of a *xoxF* deletion on P*mxa* (and P*xox*) phenocopying the effect of La^{3+} addition. Δ*xoxF* suppressor mutants offer a valuable tool to investigate the regulatory cascade. Here, we sequenced the genome of a Δ*xoxF* suppressor mutant and found a mutation in the sensor kinase gene *mxbD*. The analyzed suppressor strain showed wild type-like growth and P*mxa* expression levels on methanol in the absence of La^{3+}. If XoxF was essential for La^{3+} sensing, as suggested in the above-described model (Vu *et al.*, 2016), the addition of La^{3+} to Δ*xoxF*_sup (wild type state in absence of XoxF) should have no effect on growth and Mdh expression, respectively. Surprisingly, when La^{3+} was added, the activity of P*mxa* decreased to a minimum during growth on methanol plus succinate, while the activity of P*xox* was not affected. This finding suggests that the regulation of P*mxa* occurs in the absence of XoxF, while P*xox* autoregulation is XoxF-dependent.

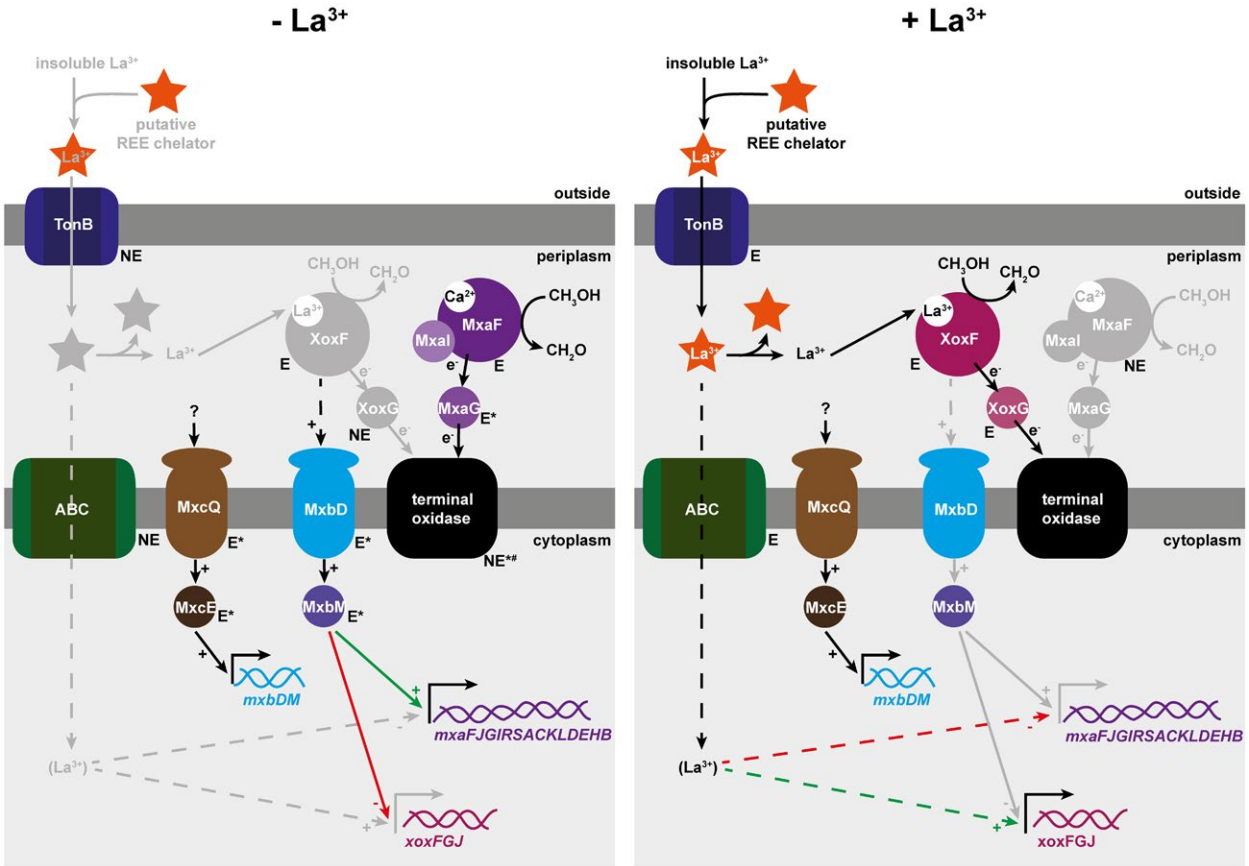

Fig. 7. Updated model of regulation of methanol dehydrogenases in *M. extorquens* in the absence (left panel) and presence (right panel) of La^{3+}. Proteins that show significantly lower abundance (fold change ≥ 4, *q*-value ≤ 0.001) under one condition are shown in gray. The essentiality of the encoding genes under the respective condition (–La^{3+} in wild type background, +La^{3+} in Δ*mxaF* background) is shown next to the proteins: E, essential; NE, nonessential; *, data taken from Ochsner et al., 2017; #, predicted redundancy. For unlabeled protein compounds, essentiality is unknown. The following abbreviations were used: TonB, Mext_1853; ABC, Mext_1846-51; MxcQ and MxcE, two-component system encoded by Mext_4452-3; MxbD and MxbM, two-component system encoded by Mext_1821-2.

In summary, these results show that a regulatory cascade lacking XoxF is still partially responsive to La^{3+}. On the one hand, this implies that La^{3+} is not only sensed via XoxF, but also by another so far unknown pathway (Fig. 7). On the other hand, this finding points towards distinct regulatory pathways for P*mxa* and P*xox*. In addition, we addressed the question whether a functional XoxF system is required for the observed regulation. A strain lacking the genes encoding XoxG and XoxJ grows normally in the absence of La^{3+}, which is in contrast to the pleiotropic effect of the corresponding deletion in *Methylomonas* sp. strain LW13 (Zheng *et al.*, 2018). Notably, the Δ*xoxGJ* strain maintained responsiveness to La^{3+}, resulting in a strong growth defect in the presence of La^{3+}. This supports the current model, where the structure of XoxF itself rather than its *in vivo* activity is important for regulation.

We show that the plant colonizer *M. extorquens* PA1 increases the amount of XoxF with increasing La^{3+} concentrations. However, both *mxaF* and *xoxF* are simultaneously expressed under La^{3+} conditions between 0.25 and 1 μM, before *mxaF* expression is fully repressed. In this context, it is interesting to note that environmental metaproteomics indicated the presence of both XoxF and MxaF under environmental *in planta* conditions (Delmotte *et al.*, 2009). The experimental system used here confirmed the presence of both MxaF and in particular XoxF during phyllosphere colonization in a gnotobiotic clay system. Plants grown under the same conditions indeed showed the presence of REEs in the phyllosphere. The concentrations measured for Y, La, Ce, Pr, Nd, and Sm in this study were between 0.5 and 10 μg g^{-1} plant dry weight. Depending on the plant species and sampling location, values previously reported in the literature are either in a similar range (Ichihashi *et al.*, 1992) or at least one order of magnitude lower (Tyler, 2004; Tyler and Olsson, 2005). The detection of both XoxF and MxaF in our experimental system is in line with observations in the environment and indicates sufficient bioavailability to induce *xoxF* expression; additionally, it provokes questions regarding the spatial repartitioning of REE *in situ*.

Apart from XoxF induction *in planta*, the proteome analyses conducted here pinpointed a few so far uncharacterized proteins that are induced by La^{3+}. Genomic context investigation of the genes encoding these proteins led to the identification of a TonB-dependent receptor and an ABC transporter that are required for REE-dependent growth on methanol (Fig. 7). The essentiality of a TonB-dependent receptor as well as the low solubility of REEs point toward a dedicated uptake mechanism involving an organic chelator analogous to siderophores for iron uptake (Wandersman and Delepelaire, 2004). The discovery of a selective chelator for REEs would have interesting applications including bioremediation of REEs-contaminated soils and recycling of REEs from technical devices.

Taken together, our results extend our knowledge of REE-dependent methylotrophy both on a molecular level and in terms of environmental significance.

Experimental procedures

Strains and growth conditions

Methylobacterium extorquens PA1 was grown at 28°C in either 3-(N-morpholino)propanesulfonic acid (MOPS)- or phosphate-buffered minimal medium. The MOPS-buffered medium contained 20 mM MOPS and 1.5 mM phosphate, 30.29 mM NH_4Cl, 0.81 mM $MgSO_4$, trace elements (10.79 μM $FeSO_4$, 40.3 μM Na_2EDTA, 15.65 μM $ZnSO_4$, 12.61 μM $CoCl_2$, 5.09 μM $MnCl_2$, 16.17 μM H_3BO_3, 1.65 μM Na_2MoO_4, 1.2 μM $CuSO_4$ and 20.41 μM $CaCl_2$), and methanol (123 mM) or succinate (30.83 mM). The phosphate-buffered medium contained 20.7 mM phosphate and otherwise identical components. Depending on the experiment, 10 μM $LaCl_3$ heptahydrate (Sigma-Aldrich, Cat#262072), YCl_3 hexahydrate (Sigma-Aldrich, Cat#464317), $GdCl_3$ hexahydrate (Sigma-Aldrich, Cat#203289), $HoCl_3$ hexahydrate (Sigma-Aldrich, Cat#289213), $YbCl_3$ hexahydrate (Sigma-Aldrich, Cat#337927), $CeCl_3$ heptahydrate (Sigma-Aldrich, Cat#202983), $NdCl_3$ hexahydrate (Sigma-Aldrich, Cat#289183), $EuCl_3$ hexahydrate (Sigma-Aldrich, Cat#203254), PrCl3 hydrate (Sigma-Aldrich, Cat#205141) or $SmCl_3$ anhydrous (Sigma-Aldrich, Cat#400610) was added. For plates, 15 g l^{-1} agar was added. *Escherichia coli* DH5α was used for molecular work and was cultured at 37°C in LB medium. If appropriate, tetracycline (10 μg ml^{-1}) or kanamycin (50 μg ml^{-1}) was added for selection.

Construction of gene deletions, expression plasmids and promoter fusions

Markerless gene deletions of *mxaF* (Mext_4150), *xoxF* (Mext_1809), Mext_1854, Mext_1806-8, Mext_1594, Mext_1595, Mext_1853, Mext_1856-7 and Mext_1848-51 were generated using pK18_*mob_sacB* (Schäfer *et al*., 1994). Deletion and subsequent replacement of *mxbD* (Mext_1821) with the suppressor version was performed using pCM433 (Marx, 2008). Plasmids for expression of *xoxF* were constructed based on pTE100 (Schada von Borzyskowski *et al*., 2014) by amplifying the *xoxF* gene including its promoter (243 bp upstream) from the *M. extorquens* PA1 genome and inserting it using the EcoRI and XbaI sites. The promoter fusion plasmid of P*xox* was constructed based on pTE100_*mChe* (Schada von Borzyskowski *et al*., 2014) by cloning 264 bp upstream of *xoxF* into the EcoRI and XbaI sites of the vector. The promoter fusion plasmid of P*mxa* was constructed based on pTE102 (Schada von Borzyskowski *et al*., 2014) by cloning the *mCherry* gene of pTE100_*mChe* into the SpeI and KpnI sites. Electrocompetent *M. extorquens* PA1 cells were prepared by incubating exponentially growing cultures (OD600 between 1 and 3) on ice for 30 min and centrifuging them at 4,000 *g* at 4°C for 15 min. The pellet was washed twice with one volume ice-cold sterile MilliQ water, followed by 0.5 volumes ice-cold sterile 10% glycerol and was finally resuspended in 0.01 volumes 10% glycerol. Competent PA1 cells were stored in 100 μl aliquots at −80°C. Electroporation of replicative plasmids into competent *M. extorquens* PA1 cells was performed at 1.8 kV, followed by regeneration in nutrient broth (NB) without NaCl (Sigma-Aldrich) at 28°C for at least 2 hours and plating on appropriate minimal medium plates. Electroporation of suicide plasmids was performed at 2.15 kV and regeneration in NB was performed for at least 5 hours before plating.

Growth assays in microtiter plates

Overnight pre-cultures were grown in 20 ml MOPS-buffered minimal medium with 30.83 mM succinate and 123 mM methanol in shake flasks. To remove the remaining substrate, cells were spun down at 3220*g* at 28°C for 15 min. The pellet was then washed with two volume equivalents of MOPS-buffered minimal medium without carbon source (MM) and resuspended in MM. Next, the OD600 was adjusted to 0.5 to inoculate the main cultures in 96-well plates (ThermoFischer Scientific Nunclon 96 Flat Bottom Transparent Polystyrol). MOPS-buffered medium (180 μl) containing the respective carbon source plus 10% to compensate for dilution by inoculation were pre-dispensed and inoculated with 20 μl of the washed culture (start OD600 = 0.05). OD600 was measured every 10 min using a Tecan Infinity M200 Pro spectrophotometer (Tecan) with a bandwidth of 9 nm and 25 flashes. The plates were shaken with 1 mm amplitude for 500 s between measurements while incubating at 28°C. Growth curves were fit using the Python-based tool croissance 1.1.0 (https://pypi.org/project/croissance/). Due to methanol evaporation, the final OD600 values should not be compared.

Promoter fluorescence assays

Fluorescence quantification was performed in a 96-well setup as described above except that black plates with a clear bottom (CELLSTAR, μClear black) in combination with a lid from a tissue culture test plate (f-base) were used; additionally, OD600 was only measured every 20 min and was followed by fluorescence measurements. The following settings were used for the fluorescence measurement: excitation at 554 nm, emission at 610 nm,

a Z-position of 17706 µm and a gain of 100. The shaking time between measurements was 870 s to accommodate the additional measurement. Fluorescence was compared at an OD600 of 0.20. The fluorescence value of the negative control (wild type plus pTE714_empty) was subtracted except if the initial fluorescence value of the well was higher than the negative control (due to promoter expression on medium used for pre-cultures, i.e. P*mxa* pre-grown on methanol without La^{3+}). In this case, the initial fluorescence values were subtracted.

Whole genome sequencing

For whole genome sequencing of Δ*xoxF*_sup, the genomic DNA was extracted using the MasterPure™ DNA and RNA Purification Kit (epicenter) and sequenced using paired-end Illumina HiSeq sequencing at the Functional Genomics Centre Zurich. Sequences were aligned to the PA1 reference genome (NC_010172.1) using the CLC Genomics Workbench 10 (Qiagen). Sanger sequencing at Microsynth (Balgach, Switzerland) confirmed the identified mutation.

Cultivation system of Arabidopsis thaliana

A. thaliana ecotype Col-0 seeds were surface sterilized and stratified at 4°C in the dark for 4 days (Innerebner *et al.*, 2011). Sterile seeds were sowed in microboxes (O118/80+OD118 filter: #40, Combiness, Nazareth, Belgium) containing calcined clay (Diamond Pro Calcined Clay Drying Agent, Arlington, USA) as described previously (Bai *et al.*, 2015). Plants were grown under gnotobiotic conditions at 22°C, 11 h light and 54% humidity in standard plant growth chambers (CU-41L4, Percival, Perry, USA). After two weeks of growth, plants were inoculated with *M. extorquens* PA1. For inoculation, bacteria were grown on minimal medium plates containing 1.5% agar, harvested and solubilized in 10 mM $MgCl_2$ and adjusted to OD600 0.007. Each plant was inoculated with 1 ml of bacteria solution or mock treated with 10 mM $MgCl_2$. Plants were harvested after 28 d of growth and the above-ground parts were carefully separated from roots using sterilized razor blades. For further processing, refer to the element analysis and proteomics parts.

Element analysis using ICP-MS

For subsequent element analysis, plants (inoculated with *M. extorquens* PA1 according to protocol above) were transferred into 2 ml screw cap micro tubes (two plants per tube, three replicates from different microboxes). The plant samples were freeze-dried in a standard freeze drier (Alpha 2-4 LD Plus, Christ, Osterode am Harz, Germany) for 60 h. Lyophilized samples were transferred into new 2 ml tubes and dry weight was measured. Samples were stored at –20°C until further processing.

Inductively coupled plasma (ICP) reference standards of lithium (Li), indium (In), uranium (U), rhodium (Rh), Y, La, Ce, Pr, Nd and Sm were purchased from VWR Chemicals, Merck KGaA Darmstadt or Inorganic Ventures and used to prepare tuning, calibration and sample solutions. Concentrated nitric acid (HNO_3, >65 wt%, purified by double sub-boiling distillation) and purified water (≥ 18.2 MΩ cm, Millipore, Billerica, USA) were used for the sample preparation. The samples were transferred into polytetrafluoroethylene (PTFE) digestion vials. HNO_3 (0.6 ml), purified water (0.2 ml) and Rh recovery standard (0.1 ml of 0.6 µg l^{-1} stock solution) were then added to all the digestion vials including the digestion blank. A microwave-assisted digestion was carried out using a turboWave (MLS GmbH, Germany) microwave system. After the complete digestion of the plant samples, the clear and colorless solutions were transferred into 50 ml centrifuge tubes (TPP, Trasadingen, Switzerland) and diluted to 10 ml using purified water. The clay samples were diluted to 20 ml using ultrapure water and the residues were filtered off using a syringe (Omnifix Braun, 10 ml, Luer) and a syringe filter (Chromafil Xtra PTFE-45/25). Prior to each measurement, the sample was further diluted and in was added as internal standard, aiming for an HNO_3 concentration of 1–2% and an In concentration of 2 µg l^{-1} in every sample. All the dilutions were prepared gravimetrically with a Mettler Toledo AT400 balance. Samples of 10 mg to 100 mg were digested and diluted 3,000 to 20,000 times.

The analysis was carried out using a sector field inductively coupled plasma mass spectrometer (Element XR, ThermoFisher, Bremen, Germany). The isotopes ^{89}Y, ^{103}Rh, ^{115}In, ^{139}La, ^{140}Ce, ^{141}Pr, ^{143}Nd, ^{146}Nd, ^{147}Sm and ^{149}Sm were measured in the low-resolution (m/Δm = 300) mode using the e-scan mode. A mass window of 130%, an integration window of 80% and an integration time of 10 ms per sample with 30 samples per peak was used in order to acquire the data, five runs and five passes were performed yielding a total measurement time of 2 min and 4 s per sample. The signal intensities of the ^{89}Y, ^{103}Rh, ^{115}In, ^{139}La, ^{140}Ce, ^{141}Pr, ^{146}Nd, ^{147}Sm isotopes were considered for the data evaluation and the quantification. The solutions were introduced using a micro-concentric nebulizer (MicroMist, 200 µl min^{-1} sample uptake rate with 1 l min^{-1} argon (Ar), glass expansion) combined with a cyclonic spray chamber (borosilicate glass, glass expansion), quartz injector, torch with guard electrode, sampler and skimmer made of nickel. A 1 µg l^{-1} tuning solution containing ^{7}Li, ^{115}In and ^{238}U was used to obtain maximum signal intensities and a flat top peak shape. The oxide formation ratio for UO/U was adjusted to <6%. Further instrumental parameters were adjusted as follows: nebulizer gas flow 1.34 l min^{-1}, coolant gas flow 16 l min^{-1}, auxiliary gas flow 0.80 l min^{-1}, RF-power 1270 W. The faraday, analog and counting detector modes were cross-calibrated using the Faraday Cross-Calibration sequence provided by the manufacturer.

An external calibration was carried out. Seven calibration solutions were measured containing 0, 0.1, 0.3, 0.5, 0.7, 0.9, 1.1 µg l^{-1} of Y, Pr, Nd, Sm ICP reference standard, 0, 0.5, 1.5, 2.0, 3.0, 4.0, 5.0 µg l^{-1} of La and Ce ICP reference standard and 0, 0.5, 1.0, 1.5, 2.0, 2.5, 3.0 µg l^{-1} of Rh ICP reference standard. A linear regression was conducted in order to fit the calibration curve. The limits of detection (LOD) were determined to be 9 pg l^{-1} for Y, 40 pg l^{-1} for La, 50 pg l^{-1} for Ce, 23 pg l^{-1} for Pr, 20 pg l^{-1} for Nd, 30 pg l^{-1} for Sm. Each value was estimated by assuming the analyte's signal

at the detection limit as the sum of the signal of the reagent blank and three times the corresponding standard deviation. Rh was used as recovery standard and a recovery of 99%–111% was determined for all the investigated samples.

Proteomics of plant-associated M. extorquens *PA1*

For recovery of *M. extorquens* PA1 from the phyllosphere of *A. thaliana*, two microboxes (corresponding to 10 plants) were transferred into 50 ml Falcon tubes containing 25 ml ice-cold TE-P buffer containing 10 mM Tris-HCl, 1 mM EDTA, 20% Percoll (Sigma-Aldrich, Buchs, Switzerland) and 0.1% Silwet L-77 (Leu+Gygax AG, Birmenstorf, Switzerland) at pH 7.5. *M. extorquens* PA1 was washed off leaves through alternating cycles of vortexing and sonication as described previously (Müller *et al*., 2016). Cell pellets were stored at −80°C until further processing. In total, three biological independent replicates were generated for MS-based proteomic analysis. As a reference, *M. extorquens* PA1 was grown on phosphate minimal medium agar plates (see above), containing 25 mM D-glucose and 123 mM methanol in the plant growth chambers at the settings described above.

Bacterial cell pellets were dissolved in lysis buffer containing 100 mM ammonium bicarbonate, 8 M urea and 1× cOmplete EDTA-free protease inhibitor cocktail (Sigma-Aldrich, Buchs, Switzerland). Bacterial cells were lysed with indirect sonication (3 × 1 min, 100% amplitude, 0.8 cycle time) in a VialTweeter (HIFU, Hielscher, Teltow, Germany). Insoluble parts were removed by centrifugation at 13,000 g for 15 min at 4°C and protein concentration of supernatant was determined using the Pierce BCA assay kit (Thermo Fischer Scientific, Reinach, Switzerland) according to the manufacturer's instructions. Protein disulfide bonds were reduced by addition of 5 mM tris(2-carboxylethyl)phosphine (TCEP, Sigma-Aldrich, Buchs, Switzerland) and incubating for 30 min at 37°C and cysteine residues were alkylated by adding 10 mM iodoacetmaide (IAA, Sigma-Aldrich, Buchs, Switzerland) and incubation for 30 min in the dark at room temperature. Samples were subsequently diluted 1:5 with freshly prepared 50 mM ammonium bicarbonate buffer to reduce the urea concentration below 2 M. Sequencing grade modified trypsin (Promega AG, Dübendorf, Switzerland) was added at an enzyme to protein ratio of 1:50 and protein digestion was carried out overnight at 37°C with shaking at 300 rpm. Subsequently, trypsin was inactivated by incubation at 95°C for 5 min and addition of formic acid to an approximate concentration of 1% followed by centrifugation at 20,000*g* for 10 min. The supernatant was desalted using Sep-Pak Vac C18 reversed phase columns (Waters Corporation, Baden-Dättswil, Switzerland) as described previously (Ochsner *et al*., 2017) and dried under vacuum. The samples were re-solubilized in 3% acetonitrile (ACN) and 0.1% formic acid (FA) to a final concentration of 0.1–1.0 mg ml^{-1}.

Mass spectrometry analysis of peptide samples was performed on an EASY-nLC 1000 system (Thermo Fischer Scientific) coupled to an Orbitrap Fusion (Thermo Fischer Scientific). The chromatographic separation was performed using an ACN/water solvent system containing two channels with 0.1% (v/v) formic acid for channel A and 0.1% (v/v) formic acid, 99.9% (v/v) acetonitrile for channel B. one micro liter of peptides were loaded on an EASY-Spray C18 LC column (75 µm × 500 mm, Thermo Fischer Scientific) heated to 50°C and eluted at a flow rate of 300 nl min^{-1} by a gradient from 2% to 5% B in 2 min, 25% B in 93 min, 35% B in 10 min and 95% B in 10 min. The mass spectrometer was configured to data-dependent acquisition and operating in top speed mode with a cycle time of 3s. Full-scan MS spectra were acquired in the Orbitrap analyzer with a mass range of 300–1500 m/z and a resolution of 120k with an automated gain control (AGC) target value of 4×10^5. HCD peptide fragments (isolation window 1.6 m/z) were obtained using a normalized collision energy of 30 with an AGC target value of 2,000 and acquired in the Ion trap with rapid scan rate. To avoid multiple scans of dominant ions, dynamic exclusion was set to 25 s. Sample measurements were acquired using internal lock mass calibration on m/z 371.10124 and 445.12003.

The raw MS files were loaded into the commercial software package Progenesis QI (Nonlinear Dynamics, v.4.0.6403.35451 using the High-Mass Accuracy Instrument option. Automatic alignment was performed using the run containing the most features, automatically chosen by Progenesis. In the aligning step, 3–5 vectors along the retention time gradient were manually seeded to aid the automatic alignment. From each Progenesis peptide ion (default sensitivity in peak picking), a maximum of the top five tandem mass spectra were exported using the charge deconvolution and deisotoping option and a maximum number of 200 peaks per MS/MS. The Mascot generic file (.mgf) was searched using the Mascot Server (Matrix Science, v.2.5.1.3) against a forward and reserved protein sequence database containing the 4829 annotated proteins of *M. extorquens* PA1 (NC_010172.1) concatenated with 6721 yeast proteins, 260 known mass spectrometry contaminants and the 11 iRT peptides. For *in planta* grown bacteria and the corresponding plate control, the TAIR database (version 10) was added to the database. Parameters for precursor ion tolerance and fragment ion tolerance were set to ± 10 ppm and ± 0.5 Da respectively. Trypsin was used as the protein cleaving enzyme, and two missed cleavages were allowed. Carbamidomethylation of cysteine was set as fixed modification, and oxidation of methionine, carbamyl of the N-terminus and lysine as variable modifications. The Mascot results were loaded into Scaffold (Proteome Software, v.4.6.1) using 5% peptide and 10% protein false discovery rate (FDR). The Scaffold Spectrum Report was exported and imported back into Progenesis QI. Normalization was performed using all proteins. For quantification, all proteins identified with at least three unique peptide ions were assessed. Proteins were grouped with Progenesis and the normalized abundance from the three most abundant peptide ions (relative quantification using Hi-3) from the same protein group were averaged together individually for each sample. For statistical testing, one-way ANOVA was applied on the normalized protein abundance. The resulting p values were corrected using the Benjamini-Hochberg correction directly in Progenesis QI. The cutoffs for significant regulation were adj. $p < 0.001$ and a log2 fold change of at least two.

Proteomics of M. extorquens *PA1 in culture*

M. extorquens PA1 was grown as independent pre- and main cultures to an OD600 1.0 ± 0.2 in liquid MOPS-buffered

minimal medium containing methanol with or without 10 μM $LaCl_3$. Subsequently, four OD600 units (corresponding to 4 ml of OD600 = 1) were sampled for each condition by spinning down for 15 min at 4°C and 3220*g*, washing with 4 ml 10 mM $MgCl_2$, resuspending in 1 ml 10 mM $MgCl_2$, spinning down again and shock-freezing the pellets in liquid nitrogen. In total, five biological independent replicates were generated for each condition.

Sample preparation and LC-MS measurements were performed as described above. The LC-MS measurements were done with a loading volume of 4 μl for each sample as well as an additional pooled sample containing equal amounts of all samples in it to create an artificial alignment reference for Progenesis QI.

Data availability

The accession number for the mass spectrometry proteomics data reported in this paper is PRIDE: PXD011842 (Vizcaino *et al*., 2016). Further data and materials will be made available upon request.

Acknowledgements

We would like to thank Catherine Aquino, Bernd Roschitzki and Jonas Grossmann from the Functional Genomics Center Zurich (FGCZ) for next-generation sequencing and support with the LC-MS/MS setup. This work was supported by a grant from the Swiss National Science Foundation Grant 31003A_173094 and ETH Zurich.

Author contributions

AMO, BH and JAV designed the research. AMO, LH, TV, RN and MBM performed the experiments. AMO, LH and TV analyzed data. AMO and JAV wrote the manuscript with input from all authors.

References

Akberdin, I.R., Collins, D.A., Hamilton, R., Oshchepkov, D.Y., Shukla, A.K., Nicora, C.D. *et al*. (2018) Rare earth elements alter redox balance in *Methylomicrobium alcliphilum* 20Z^R. *Frontiers in Microbiology*, **9**, 2735.

Amaratunga, K., Goodwin, P.M., O'Connor, C.D. and Anthony, C. (1997) The methanol oxidation genes *mxaFJGIR* (*S*) *ACKLD* in *Methylobacterium extorquens*. *FEMS Microbiology Letters*, **146**, 31–38.

Anthony, C. and Zatman, L.J. (1964) The microbial oxidation of methanol. 2. The methanol-oxidizing enzyme of *Pseudomonas* sp. M 27. *Biochemical Journal*, **92**, 614–621.

Aravind, L. and Ponting, C.P. (1999) The cytoplasmic helical linker domain of receptor histidine kinase and methyl-accepting proteins is common to many prokaryotic signalling proteins. *FEMS Microbiology Letters*, **176**, 111–116.

Arias, S., Olivera, E.R., Arcos, M., Naharro, G. and Luengo, J.M. (2008) Genetic analyses and molecular characterization of the pathways involved in the conversion of 2-phenylethylamine and 2-phenylethanol into phenylacetic acid in *Pseudomonas putida* U. *Environmental Microbiology*, **10**, 413–432.

Bai, Y., Müller, D.B., Srinivas, G., Garrido-Oter, R., Potthoff, E., Rott, M. *et al*. (2015) Functional overlap of the *Arabidopsis* leaf and root microbiota. *Nature*, **528**, 364–369.

Beek, J. ter, Guskov, A. and Slotboom, D.J. (2014) Structural diversity of ABC transporters. *The Journal of General Physiology*, **143**, 419–435.

Chistoserdova, L. (2015) Methylotrophs in natural habitats: current insights through metagenomics. *Applied Microbiology and Biotechnology*, **99**, 5763–5779.

Chistoserdova, L. (2018) Applications of methylotrophs: can single carbon be harnessed for biotechnology? *Current Opinion in Biotechnology*, **50**, 189–194.

Chistoserdova, L. and Lidstrom, M.E. (1997) Molecular and mutational analysis of a DNA region separating two methylotrophy gene clusters in *Methylobacterium extorquens* AM1. *Microbiology*, **143**, 1729–1736.

Chistoserdova, L.V. and Kalyuzhnaya, M.G. (2018) Current trends in methylotrophy. *Trends in Microbiology*, **26**, 703–714.

Chu, F., Beck, D.A.C. and Lidstrom, M.E. (2016) MxaY regulates the lanthanide-mediated methanol dehydrogenase switch in *Methylomicrobium buryatense*. *PeerJ*, **4**, e2435.

Chu, F. and Lidstrom, M.E. (2016) XoxF acts as the predominant methanol dehydrogenase in the type I methanotroph *Methylomicrobium buryatense*. *Journal of Bacteriology*, **198**, 1317–1325.

Cook, E.C., Featherston, E.R., Showalter, S.A. and Cotruvo, J.A. (2019) Structural basis for rare earth element recognition by *Methylobacterium extorquens* lanmodulin. *Biochemistry*, **58**, 120–125.

Cotruvo, J.A. Jr, Featherston, E.R., Mattocks, J.A., Ho, J.V. and Laremore, T.N. (2018) Lanmodulin: a highly selective lanthanide-binding protein from a lanthanide-utilizing bacterium. *Journal of the American Chemical Society*, **140**, 15056–15061.

Delmotte, N., Knief, C., Chaffron, S., Innerebner, G., Roschitzki, B., Schlapbach, R. *et al*. (2009) Community proteogenomics reveals insights into the physiology of phyllosphere bacteria. *Proceedings of the National Academy of Sciences USA*, **106**, 16428–16433.

Deng, Y.W., Ro, S.Y. and Rosenzweig, A.C. (2018) Structure and function of the lanthanide-dependent methanol dehydrogenase XoxF from the methanotroph *Methylomicrobium buryatense* 5GB1C. *Journal of Biological Inorganic Chemistry*, **28**, 1037–1047.

Firsching, F.H. and Brune, S.N. (1991) Solubility products of the trivalent rare-earth phosphates. *Journal of Chemical & Engineering Data*, **36**, 93–95.

Gifford, S.M., Becker, J.W., Sosa, O.A., Repeta, D.J. and Delong, F. (2016) Quantitative transcriptomics reveals the growth- and nutrient- dependent response of a streamlined marine methylotroph to methanol and naturally occurring dissolved organic matter. *mBio*, **7**, 1–15.

Good, N.M., Vu, H.N., Suriano, C.J., Subuyuj, G.A., Skovran, E. and Martinez-Gomez, N.C. (2016) Pyrroloquinoline quinone ethanol dehydrogenase in *Methylobacterium extorquens* AM1 extends lanthanide-dependent metabolism to multicarbon substrates. *Journal of Bacteriology*, **198**, 3109–3118.

Gourion, B., Rossignol, M. and Vorholt, J.A. (2006) A proteomic study of *Methylobacterium extorquens* reveals a response regulator essential for epiphytic growth. *Proceedings of the National Academy of Sciences USA*, **103**, 13186–13191.

Gu, W., Haque, M.F.U., DiSpirito, A.A. and Semrau, J.D. (2016) Uptake and effect of rare earth elements on gene expression in *Methylosinus trichosporium* OB3b. *FEMS Microbiology Letters*, **363**, 1–6.

Gu, W. and Semrau, J.D. (2017) Copper and cerium-regulated gene expression in *Methylosinus trichosporium* OB3b. *Applied Microbiology and Biotechnology*, **101**, 8499–8516.

Hider, R.C. and Kong, X. (2010) Chemistry and biology of siderophores. *Natural Product Reports*, **27**, 637.

Huang, J., Yu, Z. and Chistoserdova, L. (2018) Lanthanide-dependent methanol dehydrogenases of XoxF4 and XoxF5 clades are differentially distributed among methylotrophic bacteria and they reveal different biochemical properties. *Frontiers in Microbiology*, **9**, 1366.

Ichihashi, H., Morita, H. and Tatsukawa, R. (1992) Rare earth elements (REEs) in naturally grown plants in relation to their variation in soils. *Environmental Pollution*, **76**, 157–162.

Innerebner, G., Knief, C. and Vorholt, J.A. (2011) Protection of *Arabidopsis thaliana* against leaf-pathogenic *Pseudomonas syringae* by *Sphingomonas* strains in a controlled model system. *Applied and Environmental Microbiology*, **77**, 3202–3210.

Jahn, B., Pol, A., Lumpe, H., Barends, T.R.M., Dietl, A., Hogendoorn, C. *et al*. (2018) Similar but not the same: First kinetic and structural analyses of a methanol dehydrogenase containing a europium ion in the active site. *Chembiochem*, **19**, 1147–1153

Keltjens, J.T., Pol, A., Reimann, J. and Op den Camp, H.J. (2014) PQQ-dependent methanol dehydrogenases: rare-earth elements make a difference. *Applied Microbiology and Biotechnology*, **98**, 6163–6183.

Knief, C., Delmotte, N., Chaffron, S., Stark, M., Innerebner, G., Wassmann, R. *et al*. (2012) Metaproteogenomic analysis of microbial communities in the phyllosphere and rhizosphere of rice. *The ISME Journal*, **6**, 1378–1390.

Knief, C., Frances, L. and Vorholt, J.A. (2010) Competitiveness of diverse *Methylobacterium* strains in the phyllosphere of *Arabidopsis thaliana* and identification of representative models, including *M. extorquens* PA1. *Microbial Ecology*, **60**, 440–452.

Koebnik, R. (2005) TonB-dependent trans-envelope signalling: the exception or the rule? *Trends in Microbiology*, **13**, 343–347.

Krause, S.M.B., Johnson, T., Samadhi Karunaratne, Y., Fu, Y., Beck, D.A.C., Chistoserdova, L. *et al*. (2017) Lanthanide-dependent cross-feeding of methane-derived carbon is linked by microbial community interactions. *Proceedings of the National Academy of Sciences*, **114**, 358–363.

Lebeis, S.I., Paredes, S.H., Lundberg, D.S., Breakfield, N., Gehring, J., McDonald, M. *et al*. (2015) Salicylic acid modulates colonization of the root microbiome by specific bacterial taxa. *Science*, **349**, 860–864.

Lim, S. and Franklin, S.J. (2004) Lanthanide-binding peptides and the enzymes that Might Have Been. *Cellular and Molecular Life Sciences*, **61**, 2184–2188.

Lumpe, H., Pol, A., Op den Camp, H.J.M. and Daumann, L.J. (2018) Impact of the lanthanide contraction on the activity of a lanthanide-dependent methanol dehydrogenase – a kinetic and DFT study. *Dalton Transactions*, **47**, 10463–10472.

Martinez-Gomez, N.C., Vu, H.N. and Skovran, E. (2016) Lanthanide chemistry: from coordination in chemical complexes shaping our technology to coordination in enzymes shaping bacterial metabolism. *Inorganic Chemistry*, **55**, 10083–10089.

Marx, C.J. (2008) Development of a broad-host-range sacB-based vector for unmarked allelic exchange. *BMC Research Notes*, **1**, 1.

Masuda, S., Suzuki, Y., Fujitani, Y., Mitsui, R., Nakagawa, T., Masaki, S. *et al*. (2018) Lanthanide-dependent regulation of methylotrophy in Methylobacterium aquaticum strain 22A. *mSphere*, **3**, e00462–e00417.

McSkimming, A., Cheisson, T., Carroll, P.J. and Schelter, E.J. (2018) Functional synthetic model for the lanthanide-dependent quinoid alcohol dehydrogenase active site. *Journal of the American Chemical Society*, **140**, 1223–1226.

Morris, C.J., Kim, Y.M., Perkins, K.E. and Lidstrom, M.E. (1995) Identification and nucleotide sequences of *mxaA*, *mxaC*, *mxaK*, *mxaL*, and *mxaD* genes from *Methylobacterium extorquens* AM1. *Journal of Bacteriology*, **177**, 6825–6831.

Müller, D.B., Schubert, O.T., Röst, H., Aebersold, R. and Vorholt, J.A. (2016) Systems-level proteomics of two ubiquitous leaf commensals reveals complementary adaptive traits for phyllosphere colonization. *Molecular & Cellular Proteomics*, **15**, 3256–3269.

Nakagawa, T., Mitsui, R., Tani, A., Sasa, K., Tashiro, S., Iwama, T. *et al*. (2012) A catalytic role of XoxF1 as La^{3+}-dependent methanol dehydrogenase in *Methylobacterium extorquens* strain AM1. *PLoS One*, **7**, e50480.

Nayak, D.D. and Marx, C.J. (2014) Genetic and phenotypic comparison of facultative methylotrophy between *Methylobacterium extorquens* strains PA1 and AM1. *PLoS One*, **9**, e107887.

Noinaj, N., Guillier, M., Barnard, T.J. and Buchanan, S.K. (2010) TonB-dependent transporters: regulation, structure, and function. *Annual Review of Microbiology*, **64**, 43–60.

Nunn, D.N., Day, D. and Anthony, C. (1989) The second subunit of methanol dehydrogenase of *Methylobacterium extorquens* AM1. *Biochemical Journal*, **260**, 857–862.

Nunn, D.N. and Lidstrom, M.E. (1986) Phenotypic characterization of 10 methanol oxidation mutant classes in *Methylobacterium* sp. strain AM1. *Journal of Bacteriology*, **166**, 591–597.

Ochsner, A.M., Christen, M., Hemmerle, L., Peyraud, R., Christen, B. and Vorholt, J.A. (2017) Transposon

sequencing uncovers an essential regulatory function of phosphoribulokinase for methylotrophy. *Current Biology*, 2579–2588.

Ochsner, A.M., Sonntag, F., Buchhaupt, M., Schrader, J. and Vorholt, J.A. (2014) *Methylobacterium extorquens*: methylotrophy and biotechnological applications. *Applied Microbiology and Biotechnology*, **99**, 517–534.

Pol, A., Barends, T.R.M., Dietl, A., Khadem, A.F., Eygensteyn, J., Jetten, M.S.M. *et al*. (2014) Rare earth metals are essential for methanotrophic life in volcanic mudpots. *Environmental Microbiology*, **16**, 255–264.

Prejanò, M., Marino, T. and Russo, N. (2017) How can methanol dehydrogenase from *Methylacidiphilum fumariolicum* work with the alien Ce^{III} ion in the active center? A theoretical study. *Chemistry (Easton)*, **23**, 8652–8657.

Richardson, I. and Anthony, C. (1992) Characterization of mutant forms of the quinoprotein methanol dehydrogenase lacking an essential calcium ion. *Biochemical Journal*, **287**, 709–715.

Ryffel, F., Helfrich, E.J., Kiefer, P., Peyriga, L., Portais, J.C., Piel, J. *et al*. (2015) Metabolic footprint of epiphytic bacteria on *Arabidopsis thaliana* leaves. *The ISME Journal*, **10**, 632–643.

Schada von Borzyskowski, L., Remus-Emsermann, M., Weishaupt, R., Vorholt, J.A. and Erb, T.J. (2014) A set of versatile brick vectors and promoters for the assembly, expression, and integration of synthetic operons in *Methylobacterium extorquens* AM1 and other Alphaproteobacteria. *ACS Synthetic Biology*, **4**, 430–443.

Schäfer, A., Tauch, A., Jäger, W., Kalinowski, J., Thierbach, G. and Pühler, A. (1994) Small mobilizable multi-purpose cloning vectors derived from the *Escherichia coli* plasmids pK18 and pK19: selection of defined deletions in the chromosome of *Corynebacterium glutamicum*. *Gene*, **145**, 69–73.

Schauer, K., Rodionov, D.A. and de Reuse, H. (2008) New substrates for TonB-dependent transport: do we only see the "tip of the iceberg"? *Trends in Biochemical Sciences*, **33**, 330–338.

Schmidt, S., Christen, P., Kiefer, P. and Vorholt, J.A. (2010) Functional investigation of methanol dehydrogenase-like protein XoxF in *Methylobacterium extorquens* AM1. *Microbiology*, **156**, 2575–2586.

Schrader, J., Schilling, M., Holtmann, D., Sell, D., Filho, M., Marx, A. *et al*. (2009) Methanol-based industrial biotechnology: current status and future perspectives of methylotrophic bacteria. *Trends in Biotechnology*, **27**, 107–115.

Skovran, E. and Martinez-Gomez, N.C. (2015) Microbiology. Just add lanthanides. *Science*, **348**, 862–863.

Skovran, E., Palmer, A.D., Rountree, A.M., Good, N.M. and Lidstrom, M.E. (2011) XoxF is required for expression of methanol dehydrogenase in *Methylobacterium extorquens* AM1. *Journal of Bacteriology*, **193**, 6032–6038.

Sowell, S.M., Abraham, P.E., Shah, M., Verberkmoes, N.C., Smith, D.P., Barofsky, D.F. *et al*. (2011) Environmental proteomics of microbial plankton in a highly productive coastal upwelling system. *ISME J*, **5**, 856–865.

Springer, A.L., Morris, C.J. and Lidstrom, M.E. (1997) Molecular analysis of *mxbD* and *mxbM*, a putative sensor-regulator pair required for oxidation of methanol in *Methylobacterium extorquens* AM1. *Microbiology*, **143**, 1737–1744.

Sy, A., Timmers, A.C., Knief, C. and Vorholt, J.A. (2005) Methylotrophic metabolism is advantageous for *Methylobacterium extorquens* during colonization of *Medicago truncatula* under competitive conditions. *Applied and Environmental Microbiology*, **71**, 7245–7252.

Taubert, M., Grob, C., Howat, A.M., Burns, O.J., Dixon, J.L., Chen, Y. *et al*. (2015) XoxF encoding an alternative methanol dehydrogenase is widespread in coastal marine environments. *Environmental Microbiology*, **17**, 3937–3948.

Toyama, H., Anthony, C. and Lidstrom, M.E. (1998) Construction of insertion and deletion *mxa* mutants of *Methylobacterium extorquens* AM1 by electroporation. *FEMS Microbiology Letters*, **166**, 1–7.

Tyler, G. (2004) Rare earth elements in soil and plant systems – a review. *Plant Soil*, **267**, 191–206.

Tyler, G. and Olsson, T. (2005) Rare earth elements in forest-floor herbs as related to soil conditions and mineral nutrition. *Biological Trace Element Research*, **106**, 177–191.

Vizcaino, J.A., Csordas, A., Del-Toro, N., Dianes, J.A., Griss, J., Lavidas, I. *et al*. (2016) 2016 update of the PRIDE database and its related tools. *Nucleic Acids Research*, **44**, D447–D456.

Vogel, C., Bodenhausen, N., Gruissem, W. and Vorholt, J.A. (2016) The *Arabidopsis* leaf transcriptome reveals distinct but also overlapping responses to colonization by phyllosphere commensals and pathogen infection with impact on plant health. *New Phytologist*, **212**, 192–207.

Vorholt, J.A. (2012) Microbial life in the phyllosphere. *Nature Reviews Microbiology*, **10**, 828–840.

Vu, H.N., Subuyuj, G.A., Vijayakumar, S., Good, N.M., Martinez-Gomez, N.C. and Skovran, E. (2016) Lanthanide-dependent regulation of methanol oxidation systems in *Methylobacterium extorquens* AM1 and their contribution to methanol growth. *Journal of Bacteriology*, **198**, 1250–1259.

Wandersman, C. and Delepelaire, P. (2004) Bacterial iron sources: from siderophores to hemophores. *Annual Review of Microbiology*, **58**, 611–647.

Wehrmann, M., Berthelot, C., Billard, P. and Klebensberger, J. (2018) The PedS2/PedR2 two-component system is crucial for the rare earth element switch in Pseudomonas putida KT2440. *mSphere*, **3**, e00376–e0018.

Wehrmann, M., Billard, P., Martin-Meriadec, A., Zegeye, A. and Klebensberger, J. (2017) Functional role of lanthanides in enzymatic activity and tran scriptional regulation of pyrroloquinoline quinone- dependent alcohol dehydrogenases in Pseudomonas putida KT2440. *mBio*, **8**, 1–14.

Zheng, Y., Huang, J., Zhao, F. and Chistoserdova, L. (2018) Physiological effect of XoxG(4) on lanthanide-dependent methanotrophy. *mBio*, **9**, e02430–e02417.

Supporting Information

Additional supporting information may be found online in the Supporting Information section at the end of the article